

## Absolute Calibration of SR Interferometer by the Method of Virtual Beam Broadening

J.W. Flanagan, T. Mitsuhashi, S. Hiramatsu, KEK, Tsukuba, Ibaraki 305-0801 Japan

### Abstract

A method of performing absolute calibration of an SR interferometer has been developed which uses a weighted superposition of beam interferograms obtained over a range of beam positions at the SR source point. This method permits the absolute calibration of magnification factors in an SR interferometer beam-size measurement system using the precision of the BPM calibrations. Principles and preliminary test results from the KEKB LER are presented.

### INTRODUCTION

At KEKB, synchrotron radiation (SR) interferometers are used to measure the transverse beam sizes in both the Low Energy Ring (LER) and the High Energy Ring (HER) [1]. Deformations of the surfaces in the optical path between the beam and the interferometer slits introduce magnification errors which need to be corrected in order to measure the proper beam size. In particular, the beryllium extraction mirror surface curvature changes as a function of beam current. A means of measuring and correcting for this distortion in real-time has been developed and put into use [2][3], but an independent method of checking the absolute calibration of the SR interferometer system is needed to verify the accuracy of this correction.

One method of carrying out this calibration is to use beam size measurements taken at two different beam sizes, and solving for the calibration factor. If a beam of initial size  $\sigma_0$  is smeared over a gaussian distribution of locations of size  $\sigma_{smear}$  to make a broadened beam size  $\sigma_b$ , then the broadened beam size can be represented by adding the initial beam size and the smearing size in quadrature:

$$\sigma_b = \sqrt{\sigma_0^2 + \sigma_{smear}^2}$$

If it is assumed that the reported beam size from the interferometer differs from the true beam size by a factor  $A$ , due to magnification introduced into the system by mirror distortions, then  $\sigma'_0 = A\sigma_0$ , and  $\sigma'_b = A\sigma_b$ , where  $\sigma'_0$  is the (uncorrected) reported beam size from the interferometer for the initial beam size and  $\sigma'_b$  is that for the broadened beam size. Inserting these into the above equations gives:

$$\frac{1}{A}\sigma'_b = \sqrt{\left(\frac{1}{A}\sigma'_0\right)^2 + \sigma_{smear}^2}$$

From this, the calibration factor  $A$ , which is the ratio between the reported beam size and the true beam size becomes:

$$A = \frac{\sqrt{\sigma_b'^2 - \sigma_0'^2}}{\sigma_{smear}}$$

One method of creating a smearing of the beam that has been employed is to increase the beam emittance by a known amount by using a dispersion bump [4]. Using this method,  $\sigma_{smear}$  is calculated from the machine optics model, and thus has some model dependency in it. For the purposes of calibrating the monitor itself, it is desirable to have a method which does not depend on the optics model. Such a model-independent method of generating a precise  $\sigma_{smear}$  is described below.

### MODEL INDEPENDENT METHOD: VIRTUAL BROADENING

Instead of broadening the beam itself, we consider the creation of a "virtually broadened" beam, created by taking the superposition of multiple interferograms, each one taken with the orbit of the beam at the SR source point shifted by a different transverse offset. The justification for this comes directly from the van Cittert-Zernike theory upon which the operation of the interferometer for beam-size measurement is based. The visibility of the interference fringes from a finite source as a function of slit separation is given by the Fourier transform of the source distribution; the interference pattern observed can be treated as the superposition of many interference patterns (of visibility 1) from a distribution of point sources. The virtually broadened beam interferogram is similarly constructed from the superposition of a distribution of (finite-sized) sources.

Explicitly, we move the beam at the SR source point via transverse local bumps to a series of offset locations around the normal, unperturbed orbit. At each bump height (offset from the normal orbit)  $i$ , we record the interferogram  $I_i$  (see Fig. 1). Then we create the

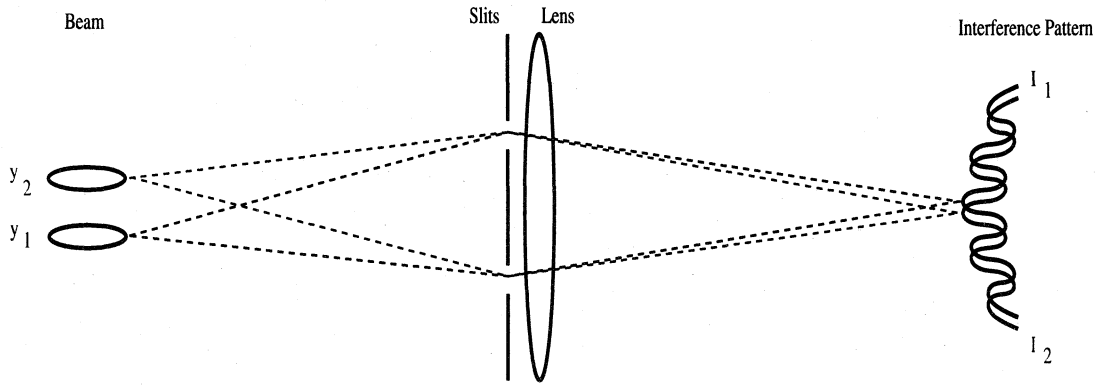


Figure 1: Beam positions and interference patterns at two different bump heights.

virtual interferogram  $I_b$  as the weighted sum of the interferograms:

$$I_b = \sum_{i=1}^n N_i I_i$$

By selecting the appropriate weighting factors  $N_i$  we can set the virtual smearing width  $\sigma_{smear}$  to be any arbitrary size. We set the  $N_i$  as follows:

$$N_i = e^{-\frac{(y_i - y_0)^2}{2\sigma_{smear}^2}}$$

where  $y_i - y_0$  is the height of the  $i$ th bump. Note that the precision of each bump height determination is determined by the precision of the BPM relative calibrations, which is  $2 - 3\mu\text{m}$  at KEKB [3], or about  $2 - 3\%$  of the vertical beam size at the SR monitor source positions.

By fitting the resulting weighted average interferogram with the same method we use for usual beam-size monitoring, we can determine  $\sigma_b$ , and hence  $A$ .

## SIMULATIONS

We did software simulations of this method, using the KEKB LER vertical interferometer spacings, using 10 bumps spaced  $50\mu\text{m}$  apart, with 1 interferograms taken at each bump height, and with  $\sigma_0 = 100\mu\text{m}$  and  $\sigma_{smear} = 75\mu\text{m}$ . (These parameters match those of the real calibration data, described in the next section.) In this case,  $\sigma_b = 125\mu\text{m}$  in the ideal case. The result of fitting the simulated virtual interferogram,  $\sigma_b(\text{fit}) = 124.881\mu\text{m}$ , shows that the virtual beam size has been created with an accuracy of  $\approx 0.1\%$ . The simulated interferograms are shown in Figs. 2 and 3.

## PRELIMINARY RESULTS

Test data were taken on 16 May 2003, using the LER vertical interferometer. Vertical position bumps

were made in 50-micron steps, from  $-600$  microns to  $+600$  microns around the regular orbit position. The raw data are shown in Figures 4 through 5. Figure 4 shows a scatterplot of reported beam sizes for several measurements at each bump height. In Figure 5, the effective slit separations at the extraction mirror are plotted for the same data. This is a measure of the magnification of the beam image due to distortions of the mirror surface [2]. In order to limit our calibration data set to raw beam images that differ systematically only in transverse offset, data taken at bump heights below  $-175$  microns and above  $380$  microns were cut. The beam sizes and mirror magnifications within the uncut regions are seen to be relatively flat. Figure 6 shows the weighting function used to create the composite virtual interferogram from the individual interferograms.

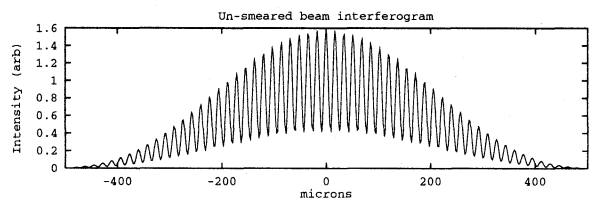


Figure 2: Simulated interferogram of real, un-broadened beam ( $\sigma_y = 100\mu\text{m}$ ).

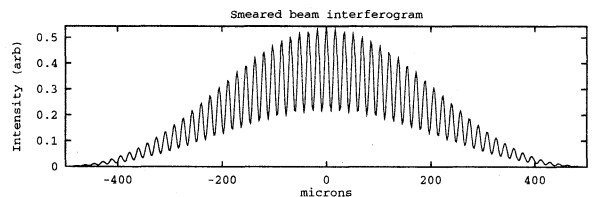


Figure 3: Simulated interferogram of virtually broadened beam ( $\sigma_{smear} = 75\mu\text{m}$ ). Note decreased visibility as a result of beam smearing, evident as a reduced peak-valley depth in the fringes.

Fitting the composite weighted sum of the histograms with the same fitting procedure used on the individual interferograms gives the result,  $A = 1.04 \pm 0.03$ . Errors include statistical errors, plus effects of changing light asymmetry between different images (1%), and orbit fluctuations and BPM scatter which lead to errors in the smearing width (1.3%). The correction of the interferometer system magnification is thus good to within the measurement accuracy of the calibration data.

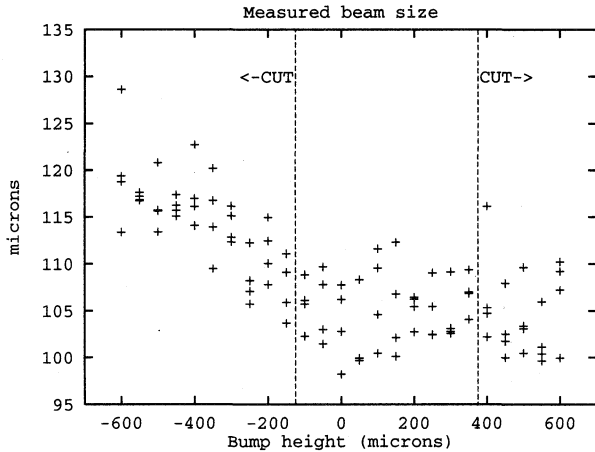


Figure 4: Bump height versus raw beam size measurements.

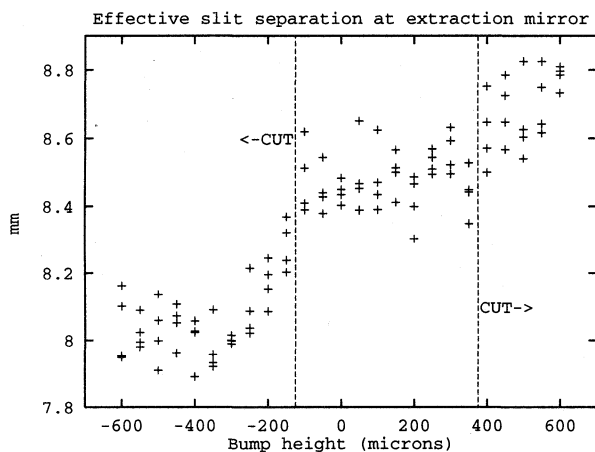


Figure 5: Bump height versus apparent slit separation on the extraction mirror surface, which is proportional to the magnification factor.

It has been pointed out that smearing in the beam position axis neglects the smearing in the transverse momentum axis that would occur if a beam were broadened physically by increasing the emittance [5]. To fully account for this effect, a two-dimensional bump scan in, and superposition over, both position and momentum axes would be needed. However, a simple way to evaluate the magnitude of the effect

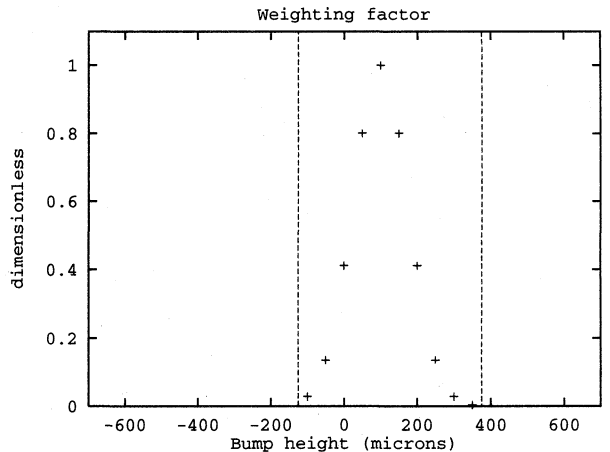


Figure 6: Weighting factors used at each bump height.

is as follows: The width of the smearing function used,  $\sigma_{smear_y}$ , is  $75\mu\text{m}$ . The corresponding momentum space width,  $\sigma_{smear_y'} = \frac{\sqrt{1+\alpha^2}}{\beta} \sigma_{smear_y}$ , is about  $6.7\mu\text{rad}$ . At the wavelength of  $500\text{ nm}$ , the vertical angular divergence of the SR beam,  $\sigma_\psi$ , is  $1.3\text{ mrad}$ . Since  $\sigma_{smear_y'} \ll \sigma_\psi$ , any deviation from symmetry in the light balance between two slits is completely negligible.

## ACKNOWLEDGMENTS

The authors wish to thank N. Iida and Y. Funakoshi for valuable discussions, particularly on their dispersion bump (“iBump”) method for cross-calibration between the interferometer and the optics model. While the principle of using measurements at two different beam sizes had been used for cross-calibrating the gated camera from the interferometer [6], they suggested its applicability to the calibration of the interferometer itself. The authors also wish to thank Prof. Kamada for discussions on the phase-space issue.

## REFERENCES

- [1] T. Mitsuhashi, J.W. Flanagan, S. Hiramatsu, “Optical Diagnostic System for the KEK B-Factory,” Proceedings of EPAC 2000, Vienna, Austria (2000) p. 1783.
- [2] J.W. Flanagan, S. Hiramatsu, H. Ikeda, T. Mitsuhashi, “Correction of Mirror Distortion Effects in Beam-Size Measurement Using SR Interferometer,” Proc. 13th Symposium on Accelerator Science and Technology, Osaka, Japan (2001), p. 381.
- [3] M. Arinaga, et al., “KEKB Beam Instrumentation Systems,” NIM A 499 (2003) pp. 100-137.
- [4] N. Iida, Y. Funakoshi, private communication.
- [5] S. Kamada, private communication.
- [6] J.W. Flanagan, et al., “High-Speed Gated Camera Observations of Transverse Beam Size along Bunch Train at the KEKB B-Factory,” Proceedings of EPAC 2000, Vienna, Austria (2000) p. 1119.